

1972), pp. 43–47. However, a larger D -state probability is favored by the Glauber theory of pion-deuteron scattering: C. Michael and C. Wilkin, Nucl. Phys. **B11**, 99 (1969).

⁵R. J. Adler and S. D. Drell, Phys. Rev. Lett. **13**, 349 (1964). See also Y. Fujii and M. Kawaguchi, Progr. Theor. Phys. **26**, 519 (1961); M. Kawaguchi and H. Yokomi, Progr. Theor. Phys., Suppl. **21**, 71 (1962); D. R. Harrington, Phys. Rev. **133**, B142 (1964).

⁶R. Blankenbecler and J. F. Gunion, Phys. Rev. D **4**, 718 (1971).

⁷M. Chemtob and M. Rho, Nucl. Phys. **A163**, 1 (1971). See also E. Kuroboshi and Y. Hara, Progr. Theor. Phys. **20**, 163 (1958), and **21**, 768 (1959). They obtained $\mu_p^{(2)} = 0.13$ nm by a Chew-Low-type calculation. Other earlier references can be found through Chemtob and Rho's paper.

⁸A. M. Green and T. H. Schucan, unpublished.

⁹H. Arenhövel and M. Danos, Phys. Lett. **28B**, 299

(1968).

¹⁰Therefore, the two-pion diagram under consideration has no contribution for isoscalar nuclei, like the deuteron and ${}^4\text{He}$.

¹¹S. Fubini, Nuovo Cimento **3**, 1425 (1956); G. Salzman, Phys. Rev. **99**, 973 (1955), and **103**, 435 (1956); F. Zachariasen, Phys. Rev. **102**, 295 (1956); S. Treiman and R. G. Sachs, Phys. Rev. **103**, 435 (1956).

¹²K. Hiida, N. Nakanishi, Y. Nogami, and M. Uehara, Progr. Theor. Phys. **22**, 247 (1959).

¹³T. Ohmura, M. Morita, and M. Yamada, Progr. Theor. Phys. **17**, 326 (1957); T. Ohmura, Progr. Theor. Phys. **22**, 34 (1959).

¹⁴J. Law and R. K. Bhaduri, Can. J. Phys. **47**, 2825 (1969).

¹⁵S. A. Moszkowski and B. L. Scott, Ann. Phys. (New York) **14**, 107 (1961).

¹⁶H. Ohtsubo, J. I. Fujita, and G. Takeda, Phys. Lett. **32B**, 82 (1970).

Experimental Study of the Decays $K_{S,L} \rightarrow \gamma\gamma^*$

M. Banner,[†] J. W. Cronin,[§] C. M. Hoffman, B. C. Knapp,^{||} and M. J. Shochet[§]

Department of Physics, Joseph Henry Laboratories, Princeton University, Princeton, New Jersey 08540

(Received 1 May 1972)

In an optical spark-chamber experiment, we measured the branching ratio $(K_S \rightarrow \gamma\gamma)/(K_S \rightarrow \text{all})$ to be $(-1.9 \pm 2.4) \times 10^{-4}$. The result assumes no interference between $K_S \rightarrow \gamma\gamma$ and $K_L \rightarrow \gamma\gamma$. We also measured the branching ratio $(K_L \rightarrow \gamma\gamma)/(K_L \rightarrow \text{all})$ to be $(4.32 \pm 0.55) \times 10^{-4} \times |\eta_{00}/\eta_{+-}|^2$.

Some recent attempts to explain the anomalously small $K_L \rightarrow \mu^+\mu^-$ branching ratio have relied upon destructive interference between the $K_2 \rightarrow \mu^+\mu^-$ amplitude and an unexpectedly large $K_1 \rightarrow \mu^+\mu^-$ amplitude.¹⁻³ It is possible that the mechanism which produces such a $K_1 \rightarrow \mu^+\mu^-$ enhancement would also produce a large $K_S \rightarrow \gamma\gamma$ decay rate. We have studied the decays $K_L \rightarrow \gamma\gamma$ and $K_S \rightarrow \gamma\gamma$ in an experiment performed in the neutral 4.7° beam at the Brookhaven alternating-gradient synchrotron. These data were collected simultaneously with data on the decays $K_{S,L} \rightarrow \pi^0\pi^0$. The $\pi^0\pi^0$ results have already been published,⁴ and the apparatus shown in Fig. 1 is also described in Ref. 4. We were able to achieve a high sensitivity to $K_S \rightarrow \gamma\gamma$ decay because the pair spectrometer had a γ -ray transverse-momentum resolution of 5 MeV/c. This enabled us to separate $\gamma\gamma$ decays from most of the dominant $2\pi^0$ background, since the γ -ray transverse-momentum spectrum from $2\pi^0$ decays cuts off at 229 MeV/c while the spectrum from the $\gamma\gamma$ mode extends up to 249 MeV/c. The K_S 's were produced by regeneration

from a K_L beam in an 8-in. uranium block. The $K_L \rightarrow \gamma\gamma$ decays which occurred downstream of the regenerator were used for normalization.

The vector momentum of one γ ray was measured in the pair spectrometer with an rms error of 2.5% in energy and 3 mrad in production angle. The decay vertex was established by the intersection of the spectrometer γ -ray trajectory with the beam which was a 0.8-in. wide by 8-in. high verti-

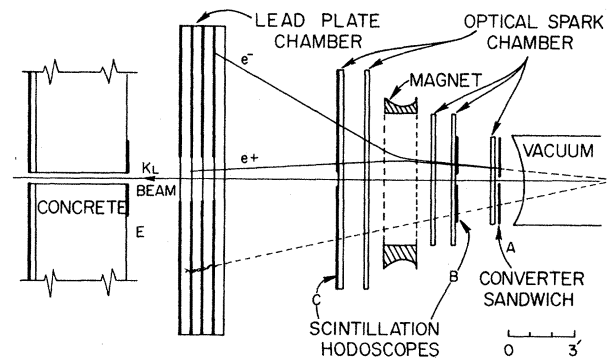


FIG. 1. Schematic view of the apparatus.

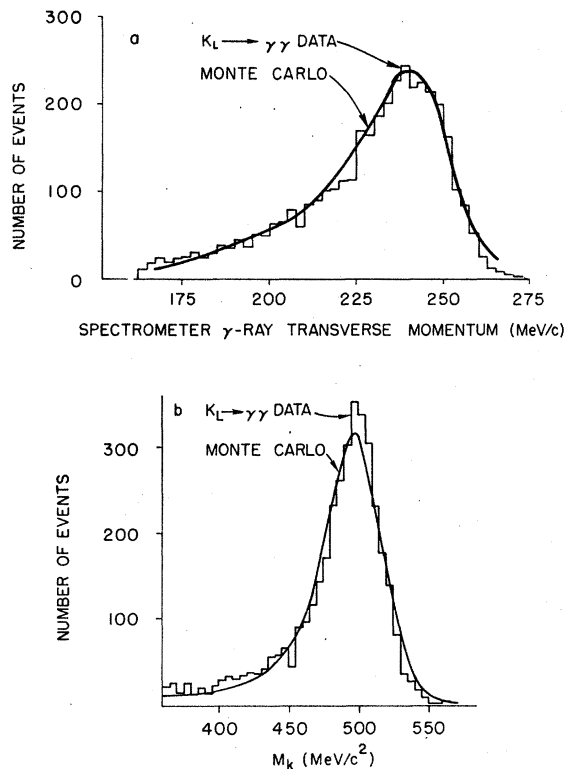


FIG. 2. $K_L \rightarrow \gamma\gamma$. (a) Spectrometer γ -ray transverse momentum and (b) reconstructed K mass. Results of Monte Carlo simulation are shown for comparison.

cal ribbon. The direction of the second γ ray was determined from its conversion in the lead-plate shower chamber and the decay vertex.

Our understanding of the apparatus was greatly aided by the presence of a strong, clean $K_L \rightarrow \gamma\gamma$ signal. From a run without the regenerator in the decay tank, we had a sample of approximately 4000 such events. Figure 2 shows the reconstructed K -mass and spectrometer γ -ray transverse-momentum spectra for these events along with similar curves from Monte Carlo simulation. The high P_\perp edge in Fig. 2(a) shows the 5-MeV/ c resolution of the apparatus.

Approximately 120 000 pictures were taken with the regenerator in the decay tank. Each spectrometer frame was measured by an automatic flying-spot scanning machine. Approximately 50% of the measured frames contained a pair of tracks which reconstructed as a γ ray. In order to reduce the number of shower chamber pictures to be measured, two cuts were then made on the data. First, the transverse momentum of the spectrometer γ ray was restricted to the range 160 to 270 MeV/ c . In addition, the decay vertex was required to be inside the decay tank. 28 000

events passed the criteria and were then measured by a group of scanners. Each event was measured independently by two scanners.

The procedure for fitting an event to the $\gamma\gamma$ hypothesis is straightforward. Since the K direction is assumed to be defined by the target and the decay point, there are only two unknowns: the K energy and the energy of the shower-chamber γ ray. The four equations expressing energy and momentum conservation thus give us two constraints. These are chosen to be the K mass and the back-to-back angle (θ_{BB}), the supplement of the angle between the two γ -ray transverse-momentum vectors. The K mass is calculated by requiring the magnitudes of the two γ -ray transverse-momentum vectors to be equal. An event was accepted as a $\gamma\gamma$ candidate if θ_{BB} was less than 150 mrad. This is 4.5 standard deviations from 0 (as determined from the $K_L \rightarrow \gamma\gamma$ data). There were 4300 such $\gamma\gamma$ candidates.

Three additional cuts were made on the $\gamma\gamma$ data in order to remove as much of the $K_S \rightarrow \pi^0\pi^0$ background as possible. First, the spectrometer γ -ray transverse momentum was required to be greater than 235 MeV/ c . This reduced the sample to 670 events. Second, events containing more than one shower-chamber track were removed. Finally, an event was removed if the shower-chamber γ -ray track ended before the middle of the last module of the chamber. This cut was made since the γ rays from $K^0 \rightarrow \gamma\gamma$ decays have a higher energy spectrum and consequently a longer mean track length than γ rays from $K^0 \rightarrow \pi^0\pi^0$ decays. We could safely make these cuts since we normalized the $K_S \rightarrow \gamma\gamma$ events to the $K_L \rightarrow \gamma\gamma$ events seen in the same run.

121 events survived these cuts. The events were of three types: $K_S^0 \rightarrow \gamma\gamma$, $K_L^0 \rightarrow \gamma\gamma$, and $K_S^0 \rightarrow \pi^0\pi^0$.⁵ Figures 3(a) and 3(b) show how the data were plotted to facilitate the separation of the various decay modes. The data were split into two bins: small back-to-back angles (0–80 mrad) and large back-to-back angles (80–150 mrad). For each bin a plot was made of the distance of the decay point from the downstream face of the regenerator (ΔZ). The presence of the K_S decays can be seen in the peaks near the regenerator, while the flat distribution far from the regenerator is due to $K_L \rightarrow \gamma\gamma$ decays. The data in each of these plots were separated into two ΔZ bins, the split being made at 35 in., which is approximately 3.5 K_S mean decay lengths (2.5 to 6.0 depending on the K momentum). The small- θ_{BB} , large- ΔZ bin should contain mostly $K_L \rightarrow \gamma\gamma$

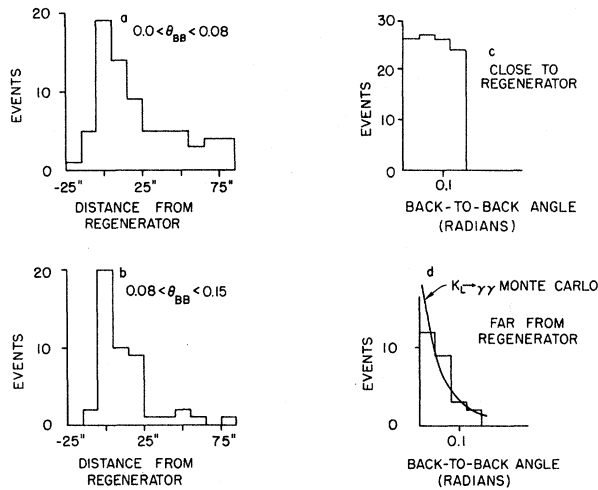


FIG. 3. Data used in the $K_S \rightarrow \gamma\gamma$ analysis. (a) Distance from the regenerator to the decay point for events with small θ_{BB} . (b) The same for events with large θ_{BB} . (c) θ_{BB} distribution for events close to the regenerator ($\Delta Z < 35$ in.), and (d) for events far from the regenerator ($\Delta Z > 35$ in.).

events, while the large- θ_{BB} , small- ΔZ bin should contain predominantly $K_S \rightarrow \pi^0\pi^0$ events. The analysis procedure then is to use these two bins to estimate the background expected in the small- θ_{BB} , small- ΔZ bin, since this is the bin which should contain most of the $K_S \rightarrow \gamma\gamma$ events.

We found 35.4 ± 6.6 $K_S \rightarrow \pi^0\pi^0$ events with $\theta_{BB} > 0.08$ and within 35 in. of the regenerator after subtracting the estimated number of $K_L \rightarrow \gamma\gamma$ events in this region. By using the flat θ_{BB} distribution for $\gamma\gamma$ fits from $K_S \rightarrow \pi^0\pi^0$ decays, a prediction of 40.5 ± 7.6 $K_S \rightarrow \pi^0\pi^0$ events was made for $\theta_{BB} < 0.08$ close to the regenerator. 20 ± 4.6 $K_L \rightarrow \gamma\gamma$ events were found in the bin with $\theta_{BB} < 0.08$ and with $\Delta Z > 35$ in. This was used with Monte Carlo results for relative efficiency versus decay-point position in the vacuum tank to give a prediction of 22.2 ± 4.9 $K_L \rightarrow \gamma\gamma$ events close to the regenerator with small θ_{BB} .

There were 53 events close to the regenerator with small θ_{BB} . As shown above, 62.7 ± 9.0 were expected from the $K_L \rightarrow \gamma\gamma$ and $K_S \rightarrow \pi^0\pi^0$ modes. Thus, -9.7 ± 11.6 were attributed to the $K_S \rightarrow \gamma\gamma$ mode. Monte Carlo calculations showed that 83.4% of all $K_S \rightarrow \gamma\gamma$ decays should have occurred in this region. Therefore, we have a total of -11.6 ± 13.9 $K_S \rightarrow \gamma\gamma$ decays. The 28.8 ± 5.7 $K_L \rightarrow \gamma\gamma$ events near the regenerator (all θ_{BB}) were used for normalization. This is the sum of the 22.2 ± 4.9 events (small ΔZ , small θ_{BB}) mentioned above, and 6.6 ± 3.0 events (small ΔZ ,

large θ_{BB}) obtained in an analogous manner from the 5.0 ± 2.2 $K_L \rightarrow \gamma\gamma$ events observed with large ΔZ and large θ_{BB} .

The validity of the branching-ratio calculation depends on the normalization events actually being $K_L \rightarrow \gamma\gamma$ decays. Figures 3(c) and 3(d) show the difference between the decays close to the regenerator (predominantly $K_S \rightarrow \pi^0\pi^0$) and those far from the regenerator (presumably $K_L \rightarrow \gamma\gamma$). The θ_{BB} distributions are shown for the two regions. Note the flat distribution for events close to the regenerator as opposed to the peaked distribution for the data far from the regenerator. Monte Carlo results for $K_L \rightarrow \gamma\gamma$ after the regenerator are shown for comparison.

An approximate value for the branching ratio (B) can be calculated by making the simplifying assumptions that the geometric acceptance for $K_S \rightarrow \gamma\gamma$ is the same as that for $K_L \rightarrow \gamma\gamma$ and that incoherent K_S regeneration and multiple K_L scattering can be ignored. The following relation can then be written:

$$\frac{N_{K_S \rightarrow \gamma\gamma}}{N_{K_L \rightarrow \gamma\gamma}} = \frac{B(K_S \rightarrow \gamma\gamma)}{B(K_L \rightarrow \gamma\gamma)} \frac{|\rho|^2}{L/\bar{\Lambda}_L},$$

where ρ is the regeneration amplitude, L is the length of the K_L decay region (35 in.), and $\bar{\Lambda}_L$ is the K_L mean decay length averaged over the K momentum spectrum (6.61×10^3 in.). It should be noted that we measured $|\rho|^2 = 0.0074 \pm 0.0005$ for the generator in another segment of this experiment.⁴ The approximate result is then $B(K_S \rightarrow \gamma\gamma) = (-1.4 \pm 1.7) \times 10^{-4}$, where we use the world average for $B(K_L \rightarrow \gamma\gamma)$. When we include the effects due to incoherent regeneration, multiple K_L scattering, and the difference between the $K_L \rightarrow \gamma\gamma$ and $K_S \rightarrow \gamma\gamma$ acceptances, we obtain the final result, $B(K_S \rightarrow \gamma\gamma) = (-1.9 \pm 2.4) \times 10^{-4}$. The probability of observing the number of events we saw or fewer is 15% for $B(K_S \rightarrow \gamma\gamma) = 0$, 10% for $B(K_S \rightarrow \gamma\gamma) = 0.5 \times 10^{-4}$, and 1.5% for $B(K_S \rightarrow \gamma\gamma) = 2.2 \times 10^{-4}$. This is approximately a factor of 10 below previously quoted values.⁶⁻⁸ The result assumes no interference between $K_L \rightarrow \gamma\gamma$ and $K_S \rightarrow \gamma\gamma$. We also considered the possibility of maximal destructive interference. For this case the probability of observing the number of events we saw or fewer is 15% for $B(K_S \rightarrow \gamma\gamma) = 6.4 \times 10^{-4}$, 10% for $B(K_S \rightarrow \gamma\gamma) = 7.1 \times 10^{-4}$, and 1.5% for $B(K_S \rightarrow \gamma\gamma) = 9.8 \times 10^{-4}$.

As mentioned previously, we detected approximately 4000 $K_L \rightarrow \gamma\gamma$ events in our run without a regenerator in the decay tank. It thus seemed natural to calculate the branching ratio for $K_L \rightarrow \gamma\gamma$. Unfortunately, there was no straightfor-

ward means of normalization. We calculated the $K_L \rightarrow \gamma\gamma$ branching ratio by using the unlikely normalization to our 120 $K_L \rightarrow \pi^0\pi^0$ events. The result is

$$B(K_L \rightarrow \gamma\gamma) = (4.32 \pm 0.55) \times 10^{-4} \times |\eta_{00}/\eta_{+-}|^2.$$

We have explicitly removed η_{00}/η_{+-} in order to separate the error due to the uncertainty in $B(K_L \rightarrow \pi^0\pi^0)$. With our measurement,⁴ $|\eta_{00}/\eta_{+-}|^2 = 1.05 \pm 0.14$, we find $B(K_L \rightarrow \gamma\gamma) = (4.54 \pm 0.84) \times 10^{-4}$. The previous world average for $B(K_L \rightarrow \gamma\gamma)$ was $(4.91 \pm 0.37) \times 10^{-4}$.^{6,9,10} Complete details on both the $K_L \rightarrow \gamma\gamma$ and $K_S \rightarrow \gamma\gamma$ results will be presented in a forthcoming article.

We would like to thank the staffs of the alternating-gradient synchrotron and the Elementary Particles Laboratory at Princeton University for their assistance. We are grateful to Walter Karp, who designed the optical system, and to Victor Bearg, who gave us a great deal of help in using the 360/91 computer. Finally, our thanks go to Sharon Unangst, who carefully handled the information flow between the scanners and the computer.

†Work supported by the U. S. Office of Naval Research and by the U. S. Atomic Energy Commission.

*This work made use of computer facilities supported in part by the National Science Foundation.

‡Present address: Département de Physique des Par-

ticules Élémentaires, Centre d'Etudes Nucléaires, Saclay, France.

[§]Present address: The Enrico Fermi Institute, University of Chicago, Chicago, Ill. 60637.

||Present address: Nevis Cyclotron Laboratory, Irvington-on-Hudson, N. Y.

¹N. Christ and T. D. Lee, Phys. Rev. D **4**, 209 (1971).

²M. K. Gaillard, Phys. Lett. **36B**, 114 (1971).

³B. R. Martin, E. de Rafael, J. Smith, and Z. E. S. Uy, Phys. Rev. D **4**, 913 (1971).

⁴M. Banner, J. W. Cronin, C. M. Hoffman, B. C. Knapp, and M. J. Shochet, Phys. Rev. Lett. **28**, 1597 (1972).

⁵Only two characteristics of $K_S \rightarrow \pi^0\pi^0$ decays were used in this analysis: the proximity of decays to the regenerator and the flat back-to-back angle distribution predicted by Monte Carlo calculations. Thus for purposes of this analysis, the $K_S \rightarrow \pi^0\pi^0$ category includes other possible regenerator-associated background.

⁶J. P. Repellin, B. Wolff, J. C. Chollet, J. M. Gaillard, M. R. Jane, and K. R. Schubert, Phys. Lett. **36B**, 603 (1971).

⁷D. Cline, W. Fry, D. Ljung, and T. Ling, "Search for the Decay $K_S^0 \rightarrow \gamma\gamma$," University of Wisconsin report, 1971 (unpublished).

⁸R. Morse, U. Nauenberg, E. Bierman, D. Sager, and A. P. Colleraine, Phys. Rev. Lett. **28**, 388 (1972).

⁹A. Rittenberg *et al.* (Particle Data Group), Rev. Mod. Phys. Suppl. **43**, 1 (1971).

¹⁰V. V. Barmin, V. G. Barylov, G. S. Veselovsky, G. V. Davidenko, V. S. Demidov, A. C. Dolgolenko, N. K. Zombkovskaya, A. G. Meshkovsky, G. S. Mirodisi, T. A. Christyakova, I. V. Chuvilo, and V. A. Shebanov, Phys. Lett. **35B**, 604 (1971).

K^- -Nucleus Scattering Lengths

Ryoichi Seki

California State University, Northridge, Northridge, California 91324

(Received 19 May 1972)

We extract K^- -nucleus scattering lengths from all K^- -mesonic atom data currently available. The scattering lengths obtained are shown to be model independent as long as the K^- -nucleus optical potential is local.

Using recently reported x-ray transitions in K^- -mesonic atoms,¹⁻³ there have been made some phenomenological studies³⁻⁶ of the K^- -nucleus optical potential. The results of the studies may be summarized as follows: (1) The potential appears to be local and proportional to the nuclear density.³ (2) Because of a large uncertainty in the strength parameter (ξ) in the potential, finding detailed structure in the nuclear density is very difficult.⁵ Of technical importance, perturbation theory is found to be inadequate because of the

large absorption effect.^{4,5}

In this Letter we report K^- -nucleus scattering lengths extracted from all K^- -mesonic atom data currently available. In contrast to the K^- -nucleus *potential*, the scattering length will be demonstrated to be practically free from the uncertainty mentioned in (2) above.

We first determine the best-fit ξ for the observed energy level and spread ΔE by numerically integrating the Klein-Gordon equation for Coulomb and strong-interaction potentials. The lat-